Measurements of the magneto-optic Kerr effect and the extraordinary Hall effect on grooved glass substrates coated with amorphous TbFeCo

S. Gadetsky, I. Syrgabaev, J. K. Erwin, and M. Mansuripur

Optical Sciences Center, University of Arizona, Tucson, Arizona 85721

T. Suzuki

IBM Almaden Research Center, 650 Harry Road, San Jose, California 95120-6099

M. Ruane

Boston University, 44 Cummington Street, Boston, Massachusetts 02215

Received March 13, 1995; revised manuscript received July 3, 1995; accepted August 7, 1995

Kerr loops measured in the 0th, −1st, and −2nd diffraction order beams on deep magneto-optic gratings show constructive and destructive interference of the beams reflected from grooves and lands as a function of effective phase depths and relative widths of grooves and lands. Hall-effect measurements yielded coercivities of grooves, lands, and sidewalls at different angles of the applied field. Sidewall reversals appear clearly in Kerr loops measured in the various diffracted beams, with signal amplitude depending on groove depth and the angle between the sidewall and the diffracted beam. © 1996 Optical Society of America

1. INTRODUCTION

The intensity and the polarization of light in the reflected diffraction orders of a coated grating depend on the period, the depth, and the shape of the grating's grooves, as well as on the properties of the coating material.[1] In the case of gratings coated with a magneto-optic (MO) material one can alter the intensity and the polarization of the diffracted beams by applying an external magnetic field, making useful applications possible. For example, MO gratings have been proposed as switches that can redirect the reflected beams when an external magnetic field is reversed.[2] Another application is erasable optical storage, where readout, focusing, and tracking signals are obtained from coated gratings (grooved MO media) containing data as magnetic domains in the coating layer. The track pitch of optical disks is typically 1.6 μm, and their groove depth is chosen to yield a (double-path) phase shift of $\pi/2$ for optimization of the characteristics of the tracking signal. Proposed higher-density media will require submicron track pitch and, possibly, periodic structures along the track for domain confinement purposes.[3] Understanding the diffraction behavior of MO gratings is therefore important both for the existing devices and for novel, emerging applications.

Design and fabrication of MO gratings are made complicated by the fact that local magnetic properties can vary from point to point when MO films are deposited onto a grooved structure. For example, the coercivity H_c can differ by as much as 2 kOe between groove and land regions in a 1 μm period grating, fabricated on a soda lime glass substrate, milled by freon ions, and coated with a thin film of TbFeCo.[3]

The present study addresses the magnetic and optical properties of deep MO gratings (i.e., those with a depth comparable with the wavelengths of visible light). Magnetization reversal in groove, land, and sidewall regions at different applied magnetic fields is observed through monitoring of the Kerr MO effect in the various diffraction orders. Also, Hall-effect measurements are used to produce estimates of the coercivities of grooves, lands, and sidewalls.

2. EXPERIMENT

Fused silica substrates were ion milled with freon ions through a striped photoresist mask exposed by two interfering coherent laser beams followed by the resist development.[4] All gratings used in this study had a 1 μm period, and in the various samples the groove depth ranged from 50 nm to 400 nm. The milled substrates were sputter coated with a multilayered MO structure: SiN (10 nm)/TbFeCo (50 nm)/SiN (80 nm). The transparent SiN layers protect the amorphous MO layer from oxidation. The TbFeCo film was Tb rich with saturation magnetization $\sim$ 200 emu/cc. Figure 1 is a scanning electron micrograph of a complete multilayer coated MO grating. The sidewalls have an angle of approximately 20° with the normal and appear to be somewhat rougher than both grooves and lands, presumably because of the nonuniform edges of the developed photoresist. The widths of lands and grooves in our samples usually differed by 5%–10%. For the specific sample shown in Fig. 1 the lands were wider.

We observed the qualitative behavior of domain structures with a polarized light microscope that used white-

0740-3232/96/020314-06$06.00

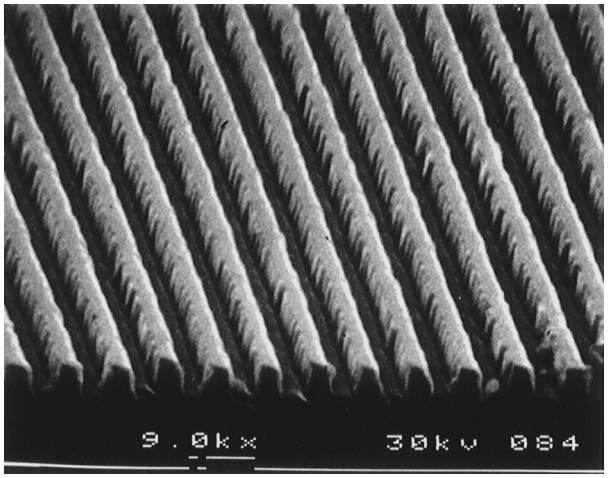

Fig. 1. Scanning electron micrograph of a 1-μm period grating coated with a multilayered magneto-optic (MO) thin film. Groove depth, from atomic force microscope measurements, is 400 nm, land width is 390 nm, and groove width is 350 nm. The angle of the sidewall is approximately 20° from the film normal.

light illumination with a 100× oil immersion objective. Images were captured as 640 × 480 pixel frames with a Vidicon camera and a personal-computer-based frame grabber. A single-pole, conical tip, ±5 kOe electromagnet, mounted under the microscope's $X-Y$ stage, allowed control of domain nucleation, growth, and contraction. At 100× grooves and lands could be distinguished as bright and dark stripes in an unprocessed image, even when the magnetization of the sample was uniformly saturated. Image processing for noise reduction, background removal, and pixel thresholding[5] was used to remove the background pattern of milled grooves and to enhance the contrast of up- and down-oriented domains.

Kerr loops were measured in a conventional loop tracer in fields up to 20 kOe and with a HeNe laser operating at $\lambda = 633$ nm.[6] The Kerr rotation angle was measured in the 0th, −1st, and −2nd order diffracted beams. We mounted samples in the loop tracer in such a way as to allow the diffracted beam to retrace its incident path to the detectors (see Fig. 2). This occurs for the mth order diffracted beam from a reflection diffraction grating when the angle θ_m between the incident beam and the grating normal satisfies the relation[7]

$$\sin\,\theta_m = m\lambda/2d\,. \tag{1}$$

In the above equation d is the period of the grating, and m is the order of the particular diffracted beam under consideration. For $d = 1$ μm and $\lambda = 633$ nm the critical angles are $\theta_m = 0°$, 18.5°, and 39.3° for the 0th, −1st, and −2nd order beams, respectively. We applied the magnetic field either parallel or perpendicular to the incident beam, thus forming the same angles with the sample (or the complement of the same angle) as those that the beam does. The polarization direction of the incident beam was always parallel to the grooves. All samples showed approximately the same Kerr rotation angle ($\theta_K \sim 0.6°$) at normal incidence in a flat area outside the grooved regions of the samples.

The average round-trip phase shift ϕ between the two beams that are retroreflected from the groove and land regions may be calculated according to the schematic shown in the inset to Fig. 2. The beams are represented by central rays striking the midpoints of the illuminated parts of the grooves and the lands (the shadowing effect is taken into account). For $\theta_m > \Psi$ simple geometrical considerations yield

$$\phi = (2\pi/\lambda)\{2h/\cos\,\theta_m + [d - h(\tan\,\Psi + \tan\,\theta_m)]\sin\,\theta_m\}, \tag{2}$$

where h is the depth of the grooves and Ψ is the angle between the sidewalls and the sample normal (in our case it is 20°). For $\theta_m \le \Psi$ we arrive at

$$\phi = (2\pi/\lambda)[2h/\cos\,\theta_m + (d - 2h\,\tan\,\theta_m)\sin\,\theta_m]. \tag{3}$$

We shall have occasion to use ϕ in our analyses of the data later in the paper.

Hall loops were measured at arbitrary orientations of the field relative to the sample normal, since there was no restriction on the geometry of the measurement system in this case. (In the case of Kerr-effect measurements the requirement that the reflected beam must return to the detectors places stringent limits on the range of available orientations.) This freedom in selecting the orientation of the field allows the magnetic field to couple more effectively with the sidewalls.

3. MAGNETO-OPTIC MEASUREMENTS

With the increasing of the applied magnetic field in the polarized light microscope domains nucleate and ex-

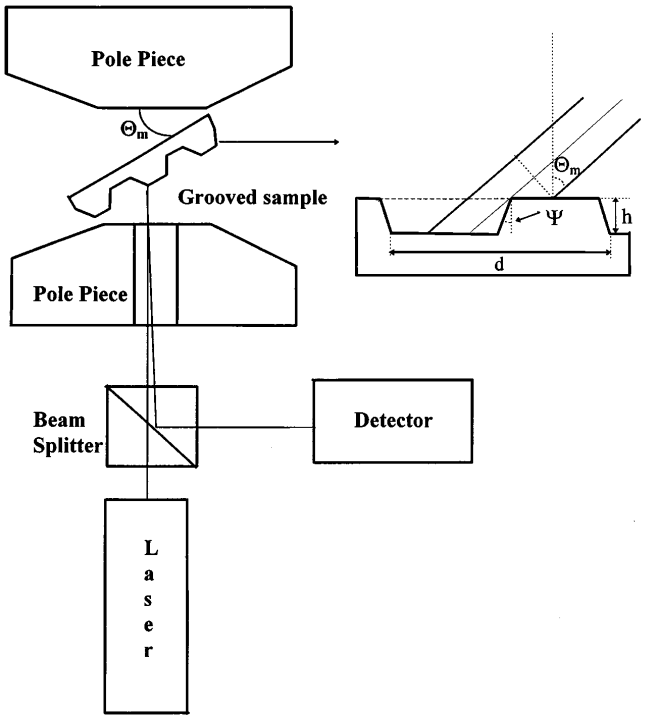

Fig. 2. Apparatus for measuring MO signal in one of the diffraction orders. The magnetic field is aligned with the direction of the incident beam. The electromagnet can also be rotated through 90° for application of a field normal to the direction of the incident beam. The inset at the upper right is a schematic drawing that shows the grating with a diffracted beam that retraces the direction of the incident beam.

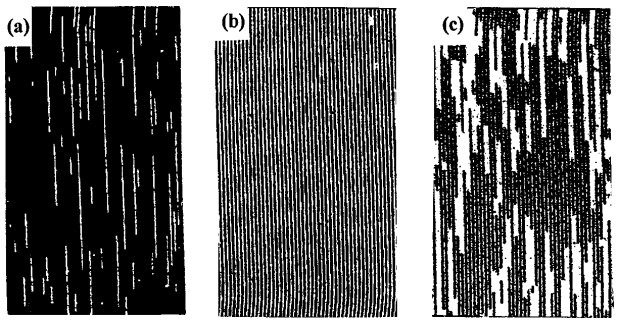

Fig. 3. Enhanced Kerr-effect micrographs showing domain reversal in a 150-nm deep, 1-μm period grating: (a) the reversed domains (white) appear in the land regions at $H = 2.8$ kOe, (b) lands completely saturate at $H = 3.3$ kOe, (c) grooves begin to reverse at $H = 4.0$ kOe. Although the same MO film coats the entire grating, its behavior resembles a two-phase system with different coercivities for the land and groove regions. The behavior of the film on the sidewalls cannot be observed in these pictures.

pand preferentially along either lands or grooves of the sample, creating images like those shown in Fig. 3. For most samples studied the coercivities of the lands and the grooves differed by several hundred oersteds, which was sufficient to allow saturation of one region before nucleation began in the other. Lower coercivity was usually found in the smoother region with fewer pinning sites. (In the case of fused-silica substrates milled by freon ions the smoother regions were the unetched lands.)

The 0th diffraction order Kerr loop for a 150 nm deep grating shows an interference effect [see Fig. 4(a)]. At $\lambda = 633$ nm 150 nm deep grooves approximately correspond to round-trip phase depths of π. A large spike is observed at the magnetic field value of $H_{\text{ext}} = -3.3$ kOe. The spike's leading edge begins with nucleation on the lower coercivity (land) areas, at approximately -2.5 kOe. The trailing edge of the spike arises as the grooves nucleate. The width of the spike is approximately 1.2 kOe. The signal does not quite return to its initial value because of the difference between groove and land widths, leaving a net imbalance. This imbalance causes the saturation value of the Kerr rotation angle to be approximately 0.2°. The spike in the positive range of the magnetic field is much smaller than that in the negative range, presumably because the stepping of the magnetic field was not fine enough to resolve this feature.

Figure 4(b) shows the MO Kerr loop measured in the -1st diffraction order of the same grating. The round-trip phase depth in this case is approximately 2π [see Eq. (2)]. No peculiarities are observed on the loop. The saturated Kerr rotation angle is approximately 0.8°, which is somewhat greater than that on a flat region of the same sample.

In Fig. 5(a) the Kerr loop measured in the 0th order for the 300 nm deep grating shows high squareness, a coercivity of nearly 3.1 kOe, and a Kerr rotation angle of 1.2°. A slight kink and change of slope are apparent above 3.3 kOe, which is characteristic of gratings with different land and groove coercivities. The kink appears at the same magnetic field as that corresponding to the spike in Fig. 4(a). Because the round-trip phase depth is nearly 2π in this case, the reflected beam from grooves is in phase with that reflected from the lands, making the Kerr loop similar to the loop expected from a flat sample. Of course, no kinks would appear in the loop from a completely flat sample with a uniform coercivity.

In Figs. 5(b) and 5(c) the 300 nm deep grating shows interference behavior in the loop obtained from the -1st and -2nd order beams, namely, a reduced saturation Kerr signal and spikes during the reversal process. The round-trip phase depth for the -1st order beam is nearly 3π, and that for the -2nd order beam is approximately 3.5π. At the peak of the spike the Kerr angle is restored from 0.1° to 0.4° in the -1st order loop and from 0.4° to 1.2° in the -2nd order loop. There is also a reversal of the sense of the loop in the -2nd order loop as compared with that of the 0th and -1st order loops. We are not able to explain the reversal of the loop sense within the frame of our model. The real behavior is more complicated, and understanding it requires a computer simulation with the use of Maxwell equations.

Interference effects are also apparent in Fig. 6(a) for the 0th order Kerr loop measured in a 400 nm deep grating. Again a reduced saturation signal and spikes between the coercive fields for the lands and the grooves are observed. The round-trip phase depth for this 0th order beam is 2.5π. The gradual change of the signal between 7 kOe and 11 kOe comes from sidewall reversal, which will be discussed further in the next section in conjunction with a description of the Hall loops measured on the same sample. The net saturation Kerr angle, which is the sum of contributions from land, groove, and sidewalls, is only 0.15°.

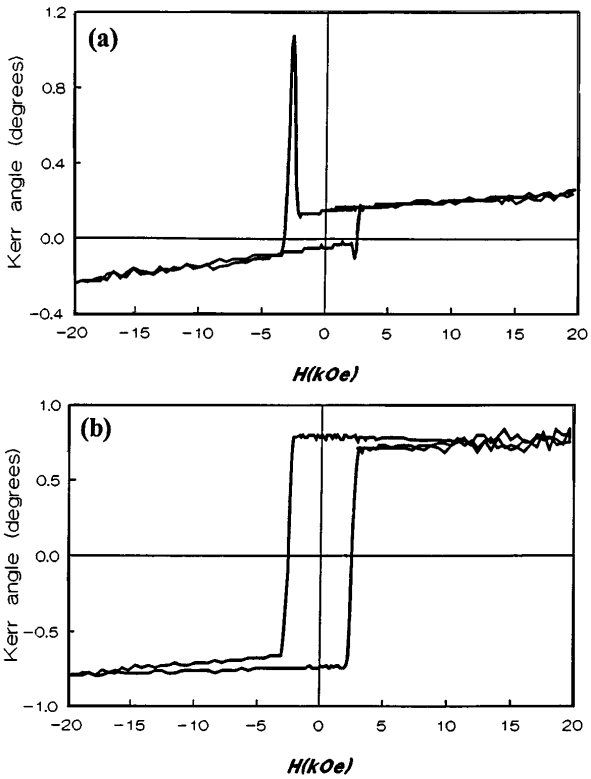

Fig. 4. Kerr MO loops for the 1 μm period grating, having a groove depth of 150 nm, measured with the use of (a) 0th order and (b) -1st order diffracted beams. The magnetic field is applied parallel to the direction of the incident beam.

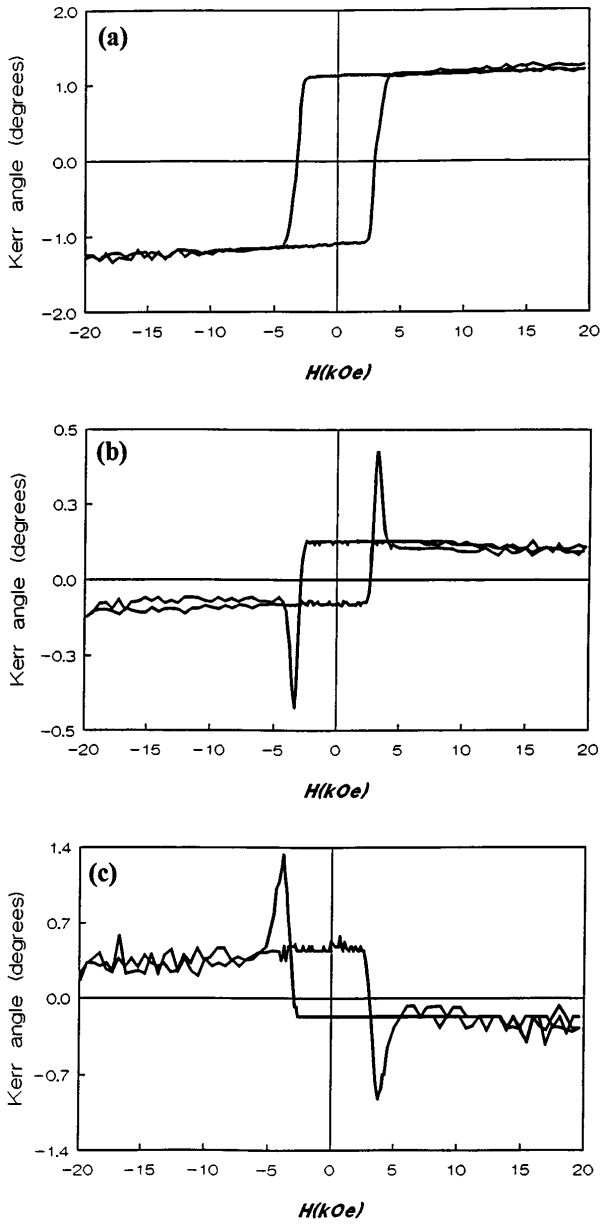

Fig. 5. Kerr MO loops measured in (a) 0th order, (b) −1st order, and (c) −2nd order diffracted beams with the magnetic field applied parallel to the incident beam. The grating period is 1 μm, and its groove depth is 300 nm.

Figure 6(b) shows the Kerr loop measured on the 400 nm deep grating in the −1st order beam. There are no sharp spikes on the loop in the vicinity of H_c, but a change of slope between 7 kOe and 9 kOe is observed. The round-trip phase depth in this case is close to 3.5π. The region with a positive slope in the field range 7 kOe to 9 kOe (or, similarly, the region with a negative slope on the opposite side of the loop) corresponds to magnetization reversal on the sidewalls. Note that sense of the loop in Fig. 6(b) is opposite to that in Fig. 6(a).

The −2nd order Kerr loop measured in the 400 nm deep grating and shown in Fig. 6(c) shows again small spikes in the vicinity of 4 kOe and a kink between 5 kOe and 7 kOe. The greater value of $H_c = 4$ kOe, observed within the grooves and the lands, is due to the obliquity of the applied magnetic field (the angle between the normal to the film surface and the direction of the field is approximately 40°). The spikes appear again because the round-trip phase depth in this case is approximately 4.5π, which is not an integer multiple of 2π. The kink separates reversal on the sidewalls from that on grooves and lands. The sense of the loop is the same as that in the flat region of the sample, but the saturation rotation of 0.5° is somewhat smaller.

Summarizing the data presented in this section, we conclude that interference effects are important when we deal with deep MO gratings. Since the magnetization reversal produces a phase shift of π in the magneto-optically generated component of polarization, any delays in the timing of the grooves reversal relative to the lands reversal can give rise to a succession of constructive and destructive interferences. If the initial round-trip phase difference ϕ, when grooves and lands are saturated in the same direction, is an integer multiple of 2π, then the MO

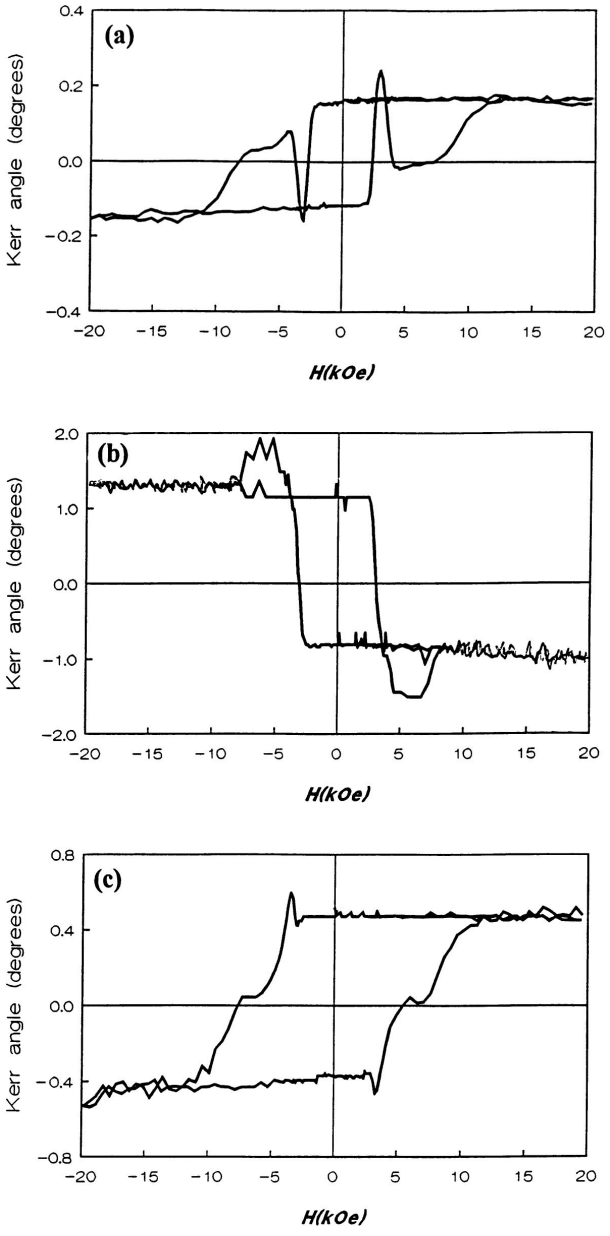

Fig. 6. Same as Fig. 5, except that the groove depth is 400 nm.

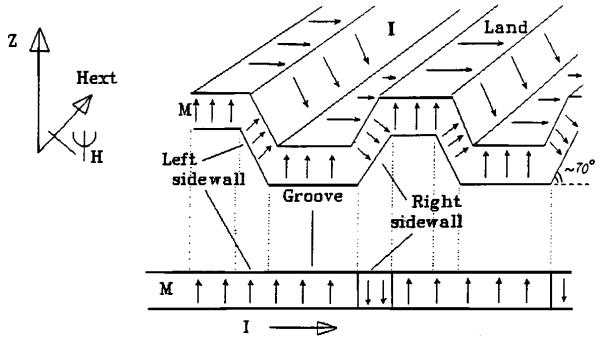

Fig. 7. Schematic diagram showing the distribution of magnetization **M** and electric current I in a thin-film grating during Hall-effect measurements. The lower part of the figure shows a projection of the cross section of the film on a flat plane when only the right sidewall has been reversed, as might occur with an applied field directed at a large angle from the Z axis.

components of oppositely magnetized grooves and lands will cancel out. This gives rise to a Kerr loop similar to that measured on the flat regions of the sample. On the other hand, if the initial round-trip phase difference is an odd multiple of π, then constructive interference of the MO component occurs when grooves and lands are oppositely magnetized. This produces a magneto-optically generated component of polarization greater than that in the fully saturated state and thus gives rise to the spikes that were observed in some of our measurements.

4. HALL-EFFECT MEASUREMENTS

In order to examine the sidewall magnetization reversal in more detail, we measured Hall loops for the 400 nm deep MO grating. Since the sidewall surface area is comparable with that of grooves and lands in this case, the Hall signal from the sidewalls is expected to be comparable with the signal from grooves and lands. The magnetic field H_{ext} was applied at different angles Ψ_H with respect to the normal to the surface of the sample. In Fig. 7 the surface arrows represent the electric current I, and the arrows in the cross section of the sample show the magnetic moment **M**. Since the extraordinary Hall effect is proportional to the component of magnetization perpendicular to the direction of current flow and since the current flow is along the film surface, the projection on the plane at the bottom of Fig. 7 may be useful for visualizing the situation.

Figure 8(a) shows the Hall loop for $\Psi_H = 0°$. Here there is a sharp change in the Hall signal corresponding to the magnetization reversal within grooves and lands near $H_{\text{ext}} = 3$ kOe. Between 5 kOe and 15 kOe the domain walls sweep through the sidewalls. The shape of the loop suggests that the Hall signal from the saturated grooves and lands is equal to the signal from the sidewalls. Therefore, at the waist of the loop, where grooves and lands are magnetized oppositely to the sidewalls, we have

$$V_{\text{Hall}} = [V_1(W_L + W_G) - 2V_2W_S]/(W_L + W_G + 2W_S) = 0. \tag{4}$$

Here W_L, W_G, and W_S are the widths of the land, groove, and sidewall regions, respectively, V_1 is the Hall voltage from the land (or the groove), and V_2 is the Hall voltage from either of the two sidewalls. The effective widths of the grooves, the lands, and the sidewalls are approximately the same for our sample, so $W_L + W_G \approx 2W_S$. Consequently, Eq. (4) yields $V_1 = V_2 = V$. This indicates that the magnetization vector is perpendicular to the surface of the film on the sidewalls. The slower rate of change of the signal above 5 kOe compared with that below arises from the fact that the field is applied at an oblique angle to the sidewall's easy axis. The fastest rate of sidewall reversal occurs near $H_{\text{ext}} = 10$ kOe. At $H_{\text{ext}} = 16$ kOe the sidewalls become saturated. When the magnetic field returns from 20 kOe to −3 kOe, the Hall signal shows a small slope. This slope indicates a

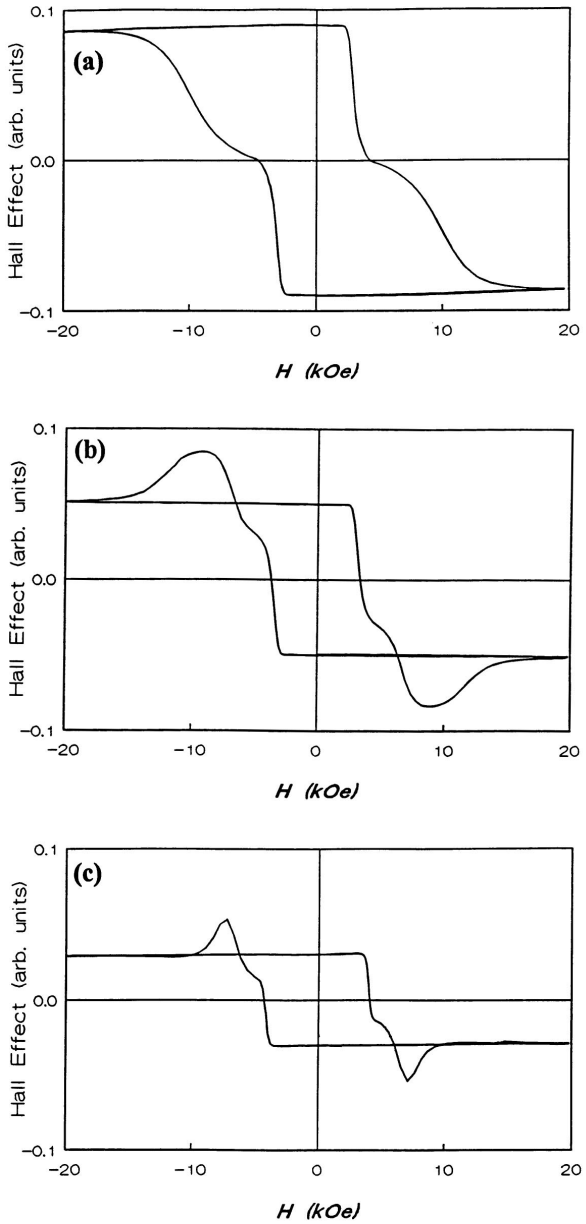

Fig. 8. Measured Hall-effect loops for a 1 μm period grating, having a groove depth of 400 nm. (a) The magnetic field is applied normal to the plane of the sample, (b) the field is applied at 40° from the Z axis, (c) the field is applied perpendicular to the left sidewall (i.e., $\Psi_H = 70°$).

deviation of sidewall magnetization from the normal direction toward the direction of the field at high fields.

The loop in Fig. 8(b) is obtained with $\Psi_H = 40°$, where the applied field makes an angle of 30° with the left sidewall normal and an angle of 70° with the right sidewall normal. When H_{ext} is directed into the left sidewall, it is also directed into the grooves and the lands but out of the right sidewall. Magnetization reversal in the right sidewall should therefore occur oppositely to that in the lands, the grooves, and the left sidewall. The slope reversal in Fig. 8(b) near 10 kOe corresponds to this opposing domain growth on the right sidewall. At $H_{\text{ext}} = 0$ the saturated grooves, lands, and sidewalls should give the following Hall voltage:

$$V_{\text{Hall}} = V(W_G + W_L)/(W_G + W_L + 2W_S) = V/2. \quad (5)$$

This is consistent with the observed ratio of the Hall signals at $H_{\text{ext}} = 0$ in Figs. 8(a) and 8(b), which is approximately 1/2. The difference between the slopes of the two sidewall signals in Fig. 8(b) arises from the fact that the angles between the left and right sidewall normals and the direction of the field are different.

Figure 8(c) shows the Hall loop obtained at $\Psi_H = 70°$, where the magnetic field is perpendicular to the left sidewall. The sharp drop near $H_{\text{ext}} = 4.5$ kOe now represents reversal within the grooves and the lands. As expected, this reversal occurs at a higher magnetic field compared with that of the case $\Psi_H = 0°$. The more gradual change of the signal near $H_{\text{ext}} = 7$ kOe indicates reversal on the left sidewall. The section of the curve with a positive slope near $H_{\text{ext}} = 9$ kOe represents magnetization reversal on the right sidewall. The total signal from the sidewall reversal in this case is smaller than that in Fig. 8(a), indicating that some of the reversals on opposite sidewalls occur at the same time, which causes partial cancellation of their Hall signals. Also, the smaller signal from lands and grooves compared with that in Fig. 8(a) implies incomplete reversal in these regions at $H_{\text{ext}} = 4.5$ kOe as a result of the obliquity of the applied magnetic field. Since the magnetic field is perpendicular to the left sidewall, the coercivity of this sidewall is estimated at 7 kOe.

5. CONCLUSIONS

Magneto-optic (MO) gratings, fabricated on fused-silica substrates, have Kerr loops in their 0th, −1st, and −2nd diffraction order beams that show interference effects. Gratings with effective phase depth of an integer multiple of 2π (double path) show little interference effect, but gratings with effective phase depth of an odd multiple of π have reduced Kerr signals in the saturated state. The Kerr signal, however, is restored when grooves and lands are saturated in opposite directions. Hall-effect measurements with an obliquely applied magnetic field yield estimates of the coercivity for the regions of grooves, lands, and sidewalls. These measurements also support interpretation of the Kerr loops in various diffraction orders in terms of land, groove, and sidewall reversals. Understanding interference effects in MO gratings will be important as more complex media designs are introduced for optical storage applications.

REFERENCES

1. M. C. Hutley, *Diffraction Gratings* (Academic, New York, 1982), Chap. 1, p. 42.
2. T. Numata, Y. Ohbuchi, and Y. Sakurai, "Stripe domain control in garnet films," IEEE Trans. Magn. **16,** 1197–1199 (1980).
3. S. Gadetsky, T. Suzuki, J. K. Erwin, and M. Mansuripur, "Domain wall pinning in amorphous TbFeCo films on patterned substrate," J. Magn. Soc. Jpn. **19,** (supplement S1), 91–96 (1995).
4. W. S. DeForest, *Photoresist Materials and Processes* (McGraw-Hill, New York, 1975), Chap. 3, p. 132.
5. B. E. Bernacki and M. Mansuripur, "Characterization of magneto-optical recording media in terms of domain boundary jaggedness," J. Appl. Phys. **69,** 4960–4962 (1991).
6. Te-ho Wu, Hong Fu, R. A. Hajjar, T. Suzuki, and M. Mansuripur, "Measurement of magnetic anisotropy constant for magneto-optical recording media: a comparison of several techniques," J. Appl. Phys. **73,** 1368–1376 (1993).
7. O. S. Heavens and R. W. Ditchburn *Insight into Optics* (Wiley, New York, 1991), Chap. 2, P. 70.